Journal of Hazardous Materials 171 (2009) 865–871

Contents lists available at ScienceDirect

Journal of Hazardous Materials

journal homepage: www.elsevier.com/locate/jhazmat

# Assessment of the biosorption characteristics of a macro-fungus for the decolorization of Acid Red 44 (AR44) dye

Tamer Akar[a,*], İlknur Tosun[a], Zerrin Kaynak[b], Emine Kavas[a], Gonul Incirkus[a], Sibel Tunali Akar[a]

[a] Department of Chemistry, Faculty of Arts and Science, Eskişehir Osmangazi University, Campus of Meşelik, 26480 Eskişehir, Turkey
[b] The Program of Chemistry, Vocational School of Higher Education, Bilecik University, 11210 Bilecik, Turkey

ARTICLE INFO

*Article history:*
Received 9 February 2009
Received in revised form 3 June 2009
Accepted 16 June 2009
Available online 23 June 2009

*Keywords:*
Biosorption
Dye
Isotherm
Kinetics
Macro-fungi

ABSTRACT

This study focuses on the possible use of macro-fungus *Agaricus bisporus* to remove Acid Red 44 dye from aqueous solutions. Batch equilibrium studies were carried out as a function of pH, biomass amount, contact time and temperature to determine the decolorization efficiency of biosorbent. The highest dye removal yield was achieved at pH 2.0. Equilibrium occurred within about 30 min. Biosorption data were successfully described by Langmuir isotherm model and the pseudo-second-order kinetic model. The maximum monolayer biosorption capacity of biosorbent material was found as $1.19 \times 10^{-4}$ mol $g^{-1}$. Thermodynamic parameters indicated that the biosorption of Acid Red 44 onto fungal biomass was spontaneous and endothermic in nature. Fourier transform infrared spectroscopy and scanning electron microscopy were used for the characterization of possible dye–biosorbent interaction and surface structure of biosorbent, respectively. Finally the proposed biosorbent was successfully used for the decolorization of Acid Red 44 in synthetic wastewater conditions.



## 1. Introduction

Contamination of water sources by dye containing wastewaters is a problem associated with industrial applications. Dye contaminated effluents can be released from many types of industries such as textile, cosmetic, craft mills, tannery, printing, pulp, paper and dye manufacturing [1]. Disposal of colored wastewaters into receiving water sources without adequate treatment causes damage to aquatic form of life and or to human beings by mutagenic and even carcinogenic effects [2].

Due to complex and stable aromatic structure of synthetic dyes, the employed existing treatment processes are generally insufficient or costly for the removal of color contaminants. These include some physical, chemical, electrochemical and biological processes [1,3]. Research interests have been focused on the development of effective and economic color removal methods. In this context biosorption is regarded as one of the popular and attractive technologies for the removal of color contaminants from aqueous media. The recent extensive studies on the application of different types of biosorbents for the decolorization purposes have been conducted by many researchers [4–10].

The use of macro-fungi type biosorbents in the biosorption process offers some technical advantages including chemical stability and good mechanical properties of biomasses in acidic and alkaline conditions. Also the fruiting bodies of macro-fungi have a tough texture structure when dried and have other physical characteristics which are conducive to their development into sorbents [11,12]. Different species of macro-fungi have been successfully used for the removal of heavy metals or dyes. Some examples are *Pycnoporus sanguineus* [13], *Phellinus badius* [11], *Fomes fomentarius*, *Phellinus igniarius* [12], *Fomitopsis carnea* [14] and *Amanita rubescens* [15].

Macro-fungus *Agaricus bisporus* is known as commercially available basidomycete. In a recent study, Ertugay and Bayhan reported the Cr(VI) biosorption potential of this macro-fungus [16]. Also the species *A. macrosporus* have been successfully used to remove heavy metals in compost (solid substrate) [17] and in effluents (contaminated solutions) [18]. In our previous studies we reported the combined actions of *A. bisporus* and *Thuja orientalis* cones for reactive dye removal from aqueous solutions [19,20].

As far as we are aware, there are to date no studies available in the literature regarding the biosorption potential of this biomass in its natural form for acid dye removal. Therefore, this study is focused on the biosorption characterization of *A. bisporus* in native form for the removal of an acid dye Acid Red 44 (AR44) from aqueous solutions. Effects of initial pH, biomass amount, contact time and temperature on the batch biosorption performance of biomass were tested. Biosorption behavior of biomass was investigated by means of different kinetic and isotherm models. In addition, mechanism of the biosorption was examined. Moreover the possible

* Corresponding author. Tel.: +90 222 2393750/2871; fax: +90 222 2393578.
*E-mail address:* takar@ogu.edu.tr (T. Akar).

0304-3894/$ – see front matter © 2009 Elsevier B.V. All rights reserved.
doi:10.1016/j.jhazmat.2009.06.085

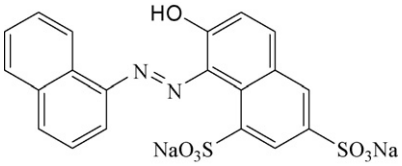


**Fig. 1.** Chemical structure of AR44 dye.

use of the biosorbent in synthetic wastewater conditions was also explored.

## 2. Materials and methods

### 2.1. Biosorbent material and dye solutions

Fresh fungal biomass of *A. bisporus* was obtained from a commercial company. Fruiting bodies of fungi was cleaned by washing repeatedly with deionized water and dried at 80 °C for 24 h. Dried biomass was crushed and sieved through an 150 μm ASTM Standard sieve to obtain uniform particle size and then stored in glass bottles prior to use. The Acid Red 44 (MW 502.43) dye, obtained from Sigma–Aldrich Corporation, St. Louis, MO, USA, was used without further purification. The chemical structure of dye was included in Fig. 1. A stock solution (1.0 g $L^{-1}$) of dye was prepared by dissolving appropriate amount of dye in deionized water and the other concentrations were obtained by diluting this stock dye solution. The pH adjustment of the working solutions was made by adding 0.1 M HCl and/or 0.1 M NaOH solutions.

### 2.2. Biosorption studies

The batch equilibrium process was used to characterize the biosorption ability of fungal biomass. 100 mL beakers containing 50 mL of dye solutions were magnetically stirred at 200 rpm using a digitally controlled magnetic stirrer. In order to determine the optimum biosorption conditions, which enhance the AR44 biosorption, experiments were performed in the pH range of 1.0–10.0, biosorbent concentration, from 0.4 to 4.0 g $L^{-1}$, contact time from 10 to 120 min and initial dye concentration from 50 to 300 mg $L^{-1}$. At the end of the experiments biosorbent–dye mixtures were centrifuged at 4500 rpm for 3 min and the supernatants were analyzed to determine the residual AR44 concentration. The biosorption kinetics of AR44 was examined by analyzing the dye biosorption within the time range of 10–120 min and at different temperatures (20, 30 and 40 °C).

The dye biosorption capacity was determined by using the following general mass-balance equation:

$$q_e = \frac{V(C_i - C_e)}{m} \quad (1)$$

where $C_i$ and $C_e$ are the initial and equilibrium concentrations of dye mol $L^{-1}$, respectively; $V$ is the volume of the dye solution (L) and $m$ is the amount of biosorbent used (g).

The influence of the matrix effect on the biosorption performance of the biosorbent was also tested at optimum conditions. Experiments were conducted with synthetic wastewater samples containing AR44 and different constituents.

### 2.3. Analysis

The remaining dye concentration in the supernatant was analyzed using a UV/visible spectrophotometer (Shimadzu UV-2550) at maximum wavelengths ($\lambda_{max}$) of 510 nm. FTIR spectra of virgin and dye-loaded biosorbent were recorded by PerkinElmer spectrum100 spectrophotometer in the region of 400–4000 $cm^{-1}$. Zeta potential measurements of the biomass were performed on Malvern Zeta sizer instrument. The surface morphology of the biomass was examined by scanning electron microscopy (Jeol 560 LV SEM) at 20 kV and 1000× magnification.

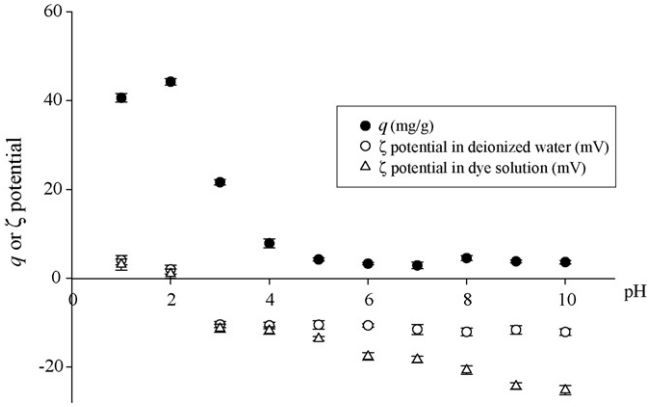


**Fig. 2.** Biosorption pattern of *A. bisporus* for AR44 and ζ potentials of the biomass in deionized water and dye solution as a function of pH (the bars represent the standard error of the mean).

## 3. Results and discussion

### 3.1. Effect of medium pH

pH is one of the important parameters affecting the biosorption potential of biosorbent material. The biosorption pattern of *A. bisporus* in the pH range of 1.0–10.0 was given in Fig. 2. As expected, high biosorption yield was observed in acidic pH values. The biosorption capacity decreased from 44.23 at pH 2.0 to 3.61 mg $g^{-1}$ at pH 10.0. This observation was in agreement with the previous findings about biosorption of Acid Blue 161 [21] and Reactive Brilliant Red K-2BP [22]. The biosorbent surface contains different functional groups and these binding groups give a net charge at different pH values. The high biosorption observed at acidic pH values can be attributed to interaction of negatively charged dye molecules and positively charged binding sites on the biosorbent surface. A decrease in the biosorption yield with increasing pH can be explained by the electrostatic repulsive forces between the deprotonated binding sites and dye anions. The surface charge of the biomass varied from +4.06 to −12.15 mV when the pH was changed from 1.0 to 10.0 (Fig. 2). These results agree with the biosorption trend for AR44 onto *A. bisporus* as a function of pH. The isoelectric point of the biomass was around 2.5. On the other hand AR44 dye molecules in the medium slightly modified the zeta potential pattern of the biomass. This can be explained by the biosorption of AR44 onto *A. bisporus* biomass.

### 3.2. Effect of biosorbent amount

Fig. 3 illustrates a plot of the biosorption yield versus biosorbent amount. As the biosorbent dosage increases, from 0.4 to 3.0 g $L^{-1}$, the percentage biosorption of AR44 was increased from 13.0% to 95.24% and then remains almost constant. So, the biosorbent amount of 3.0 g $L^{-1}$ was chosen for the further experiments. The linear increase in the biosorption yield can be explained by the increased surface area of the biosorbent and availability of more binding sites for dye molecules [23]. Further constant biosorption trend may be explained by the saturation of the dye binding sites on the biosorbent surface and establishment of equilibrium between the dye molecules to bind the biosorbent surface and those remaining in the biosorption medium. Similar trend of biomass dosage effect was observed for Basic Blue 9 and Basic Red 5 biosorption on

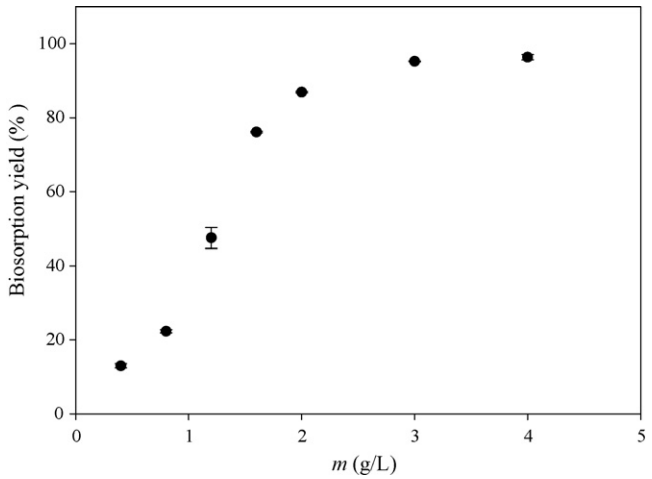


**Fig. 3.** Effect of the biosorbent amount ($m$) on the biosorption of AR44 onto *A. bisporus* (the bars represent the standard error of the mean).

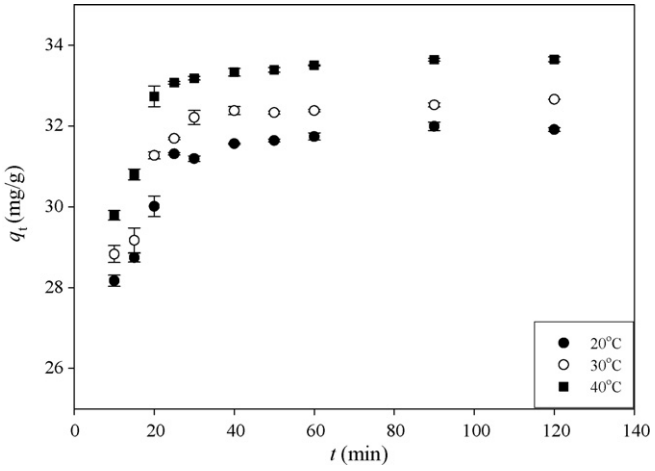


**Fig. 4.** Effect of the contact time on the biosorption of AR44 onto *A. bisporus* at various temperatures (the bars represent the standard error of the mean).

modified rice straw [24] and basic yellow biosorption on a macroalgae *Caulerpa scalpelliformis* [5].

### 3.3. Effect of temperature and contact time

Fig. 4 shows the effect of the temperature on AR44 biosorption as a function of contact time. The results indicated that rapid dye removal phase within the first 15 min was followed by equilibrium at all studied temperatures. Also it can be seen that the equilibrium biosorption capacity of *A. bisporus* increased from 31.31 to 33.07 mg g$^{-1}$ when the temperature was increased from 20 to 40 °C. An increase in dye removal capacity of the biomass with temperature indicates the biosorption of AR44 dye on macro-fungus *A. bisporus* is kinetically controlled by an endothermic process.

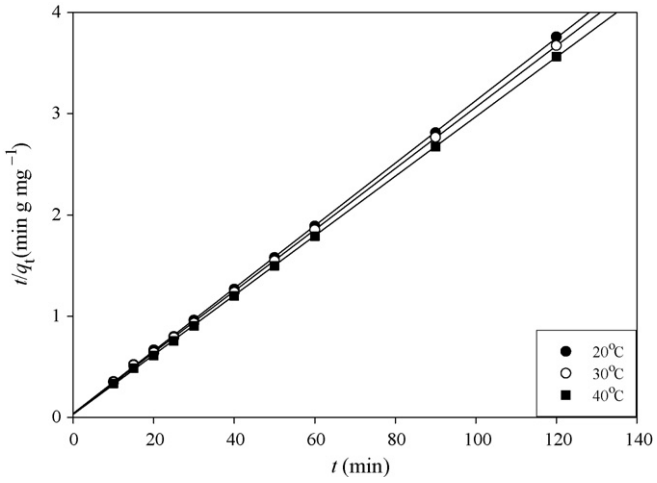


**Fig. 5.** Pseudo-second-order kinetic plots for the biosorption of AR44 onto *A. bisporus* at various temperatures.

### 3.4. Biosorption kinetics and isotherm modeling

The equilibrium and the kinetics of a sorption process provide more important data for the evaluation of sorption process as a unit operation [25]. The Lagergren pseudo-first-order and the pseudo-second-order models were chosen to analyze the kinetic behavior of biosorbent.

The Lagergen pseudo-first-order rate expression [26] is expressed as

$$\ln(q_e - q_t) = \ln\ q_e - K_L t \quad (2)$$

The pseudo-second-order kinetic equation [27] is expressed as

$$\frac{t}{q_t} = \frac{1}{k_2 q_2^2} + \frac{1}{q_2} t \quad (3)$$

where $q_e$ and $q_t$ are the biosorption capacities of biosorbent at equilibrium, and time $t$ (mg g$^{-1}$), respectively. $K_L$ is the rate constant for pseudo-first-order biosorption (1 min$^{-1}$). $q_2$ is the maximum biosorption capacity (mg g$^{-1}$) for the pseudo-second-order biosorption, $k_2$ is the equilibrium rate constant of pseudo-second-order biosorption (g mg$^{-1}$ min$^{-1}$).

The rate parameters presented in Table 1 have been obtained from the straight line plots of $\ln(q_e - q_t)$ versus $t$ for the Lagergren pseudo-first-order model (figure not shown) and $t/q_t$ versus $t$ for the pseudo-second-order model (Fig. 5). According to $r^2$ values in Table 1, the pseudo-second-order kinetic model showed satisfactory fits. The $q_2$ values estimated from the pseudo-second-order kinetic model were also good agreement with the experimental values at all temperatures studied. These findings indicated that the pseudo-second-order kinetic model is more suitable to describe the AR44 biosorption onto *A. bisporus*.

In order to evaluate the equilibrium data in this study, the Freundlich [28], Langmuir [29], and Dubinin–Radushkevich (D–R) [30] isotherm models (Eqs. (4)–(6)) were employed. According to Freundlich model, adsorption process occurs on heterogeneous surfaces and the adsorption capacity is related to the concentration

**Table 1**
Kinetic parameters for the biosorption of AR44 onto *A. bisporus* at various temperatures.

| $T$ (°C) | $q_{exp}$ (mg g$^{-1}$) | Pseudo-first-order kinetic model | | | Pseudo-second-order kinetic model | | |
|---|---|---|---|---|---|---|---|
| | | $K_L$ (min$^{-1}$) | $q_e$ (mg g$^{-1}$) | $r_1^2$ | $k_2$ (g mg$^{-1}$ min$^{-1}$) | $q_{e,cal}$ (mg g$^{-1}$) | $r_2^2$ |
| 20 | 31.31 | $3.41 \times 10^{-2}$ | 2.85 | 0.831 | $2.36 \times 10^{-2}$ | 32.41 | 0.999 |
| 30 | 31.69 | $4.08 \times 10^{-2}$ | 3.16 | 0.783 | $2.48 \times 10^{-2}$ | 33.03 | 0.999 |
| 40 | 33.07 | $6.70 \times 10^{-2}$ | 5.18 | 0.948 | $2.94 \times 10^{-2}$ | 33.99 | 0.999 |

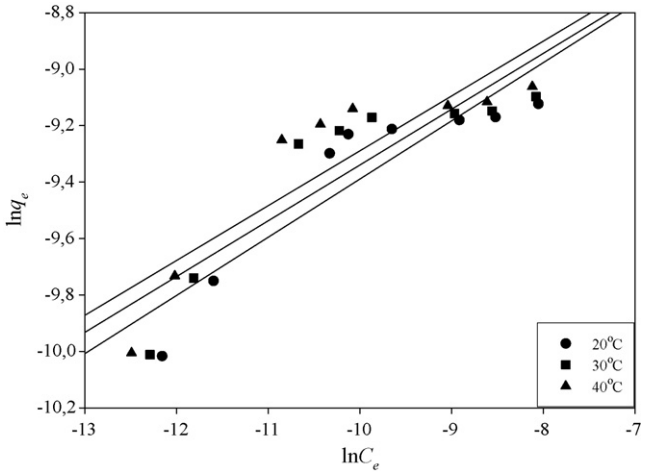


**Fig. 6.** Freundlich isotherm plots for the biosorption of AR44 onto *A. bisporus* at various temperatures.

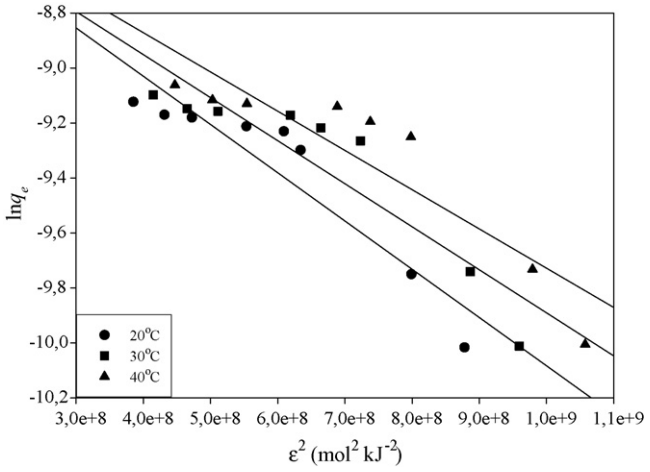


**Fig. 8.** D–R isotherm plots for the biosorption of AR44 onto *A. bisporus* at various temperatures.

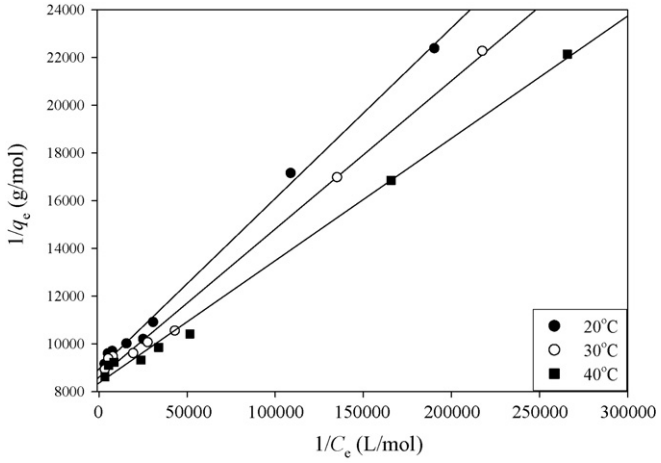


**Fig. 7.** Langmuir isotherm plots for the biosorption of AR44 onto *A. bisporus* at various temperatures.

of solute at equilibrium. The Langmuir theory assumes a homogeneous type of sorption. It is meaning that once a dye molecule occupies a binding site, no further adsorption can take place at that site. The D–R isotherm model is more general than the Langmuir isotherm. It was applied to distinguish the nature of biosorption as physical or chemical [31]. The linearized forms of the model equations are given below:

$$\ln\ q_e = \ln K_F + \frac{1}{n}\ln C_e \tag{4}$$

$$\frac{1}{q_e} = \frac{1}{q_{max}} + \left(\frac{1}{q_{max}K_L}\right)\frac{1}{C_e} \tag{5}$$

$$\ln\ q_e = \ln q_m - \beta\varepsilon^2 \tag{6}$$

In Eq. (4) $q_e$ (mol g$^{-1}$) and $C_e$ (mol L$^{-1}$) are the dye equilibrium concentrations in the solid and liquid phases; $K_F$ (L g$^{-1}$) and $n$ (dimensionless) are characteristic constants that indicate the extent of the biosorption, and the degree of nonlinearity between solution concentration and biosorption, respectively. The values of $K_F$ and $1/n$ are determined from the intercept and slope of the Freundlich plots (Fig. 6).

In Eq. (5) $q_{max}$ is the monolayer biosorption capacity of the biosorbent (mol g$^{-1}$); and $K_L$ is the Langmuir constant (L mol$^{-1}$), and is related to the free energy of biosorption. A plot of $1/q_e$ versus $1/C_e$ for the biosorption of AR44 onto *A. bisporus* (Fig. 7) shows a straight line of slope, $1/q_{max}\,K_L$, and intercept, $1/q_{max}$.

In Eq. (6) $\varepsilon$ is Polanyi potential, $q_m$ is the theoretical saturation capacity of biomass (mol g$^{-1}$), $\beta$ is the constant related to the biosorption energy. By plotting ln $q_e$ versus $\varepsilon^2$ (Fig. 8), it is possible to determine the value of $q_m$ (mol g$^{-1}$) from the intercept, and the value of $\beta$ from the slope.

The determined parameter values for the isotherm models are given in Table 2. It can be seen from Table 2 that, the numerical values of the Freundlich constant $n$ were between 4.850 and 5.149. Values of $n$ greater than unity indicate that dye anions are favorably biosorbed [32] by *A. bisporus* at all of the temperatures studied. The Langmuir model has high $r^2$ values indicating the formation of a monolayer of AR44 covering the *A. bisporus* surface. The maximum monolayer biosorption capacities were found as $1.12 \times 10^{-4}$ mol g$^{-1}$ (56.27 mg g$^{-1}$), $1.16 \times 10^{-4}$ mol g$^{-1}$ (58.28 mg g$^{-1}$) and $1.19 \times 10^{-4}$ mol g$^{-1}$ (59.80 mg g$^{-1}$) at the temperatures of 20, 30 and 40 °C, respectively. These values agreed with the experimental results.

The Langmuir constant, $K_L$, can be used to determine the suitability of the biosorbent for the sorbate using the Hall separation factor ($R_L$, dimensionless) as follows [33,34]:

$$R_L = \frac{1}{1 + K_L C_o} \tag{7}$$

where $C_o$ is the highest initial dye concentration (mol L$^{-1}$). $R_L$ values can be used for the interpretation of the sorption type and if $R_L$

**Table 2**
Biosorption isotherm constants for the biosorption of AR44 onto *A. bisporus* at various temperatures.

| $T$ (°C) | $q_{exp}$ (mol g$^{-1}$) | Langmuir constants | | | | Freundlich constants | | | Dubinin–Radushkevich (D–R) constants | | | |
|---|---|---|---|---|---|---|---|---|---|---|---|---|
| | | $q_{max}$ (mol g$^{-1}$) | $K_L$ (L mol$^{-1}$) | $r^2_L$ | $R_L$ | $n$ | $K_F$ (L g$^{-1}$) | $r^2_F$ | $q_m$ (mol g$^{-1}$) | $\beta$ (mol$^{-2}$ kJ$^{-2}$) | $r^2_{D-R}$ | $E$ (kJ mol$^{-1}$) |
| 20 | $1.09 \times 10^{-4}$ | $1.12 \times 10^{-4}$ | $1.25 \times 10^{5}$ | 0.996 | $1.32 \times 10^{-2}$ | 4.850 | $6.57 \times 10^{-4}$ | 0.826 | $2.42 \times 10^{-4}$ | $1.32 \times 10^{-3}$ | 0.867 | 19.46 |
| 30 | $1.12 \times 10^{-4}$ | $1.16 \times 10^{-4}$ | $1.39 \times 10^{5}$ | 0.994 | $1.19 \times 10^{-2}$ | 5.059 | $6.34 \times 10^{-4}$ | 0.786 | $2.43 \times 10^{-4}$ | $1.25 \times 10^{-3}$ | 0.830 | 20.00 |
| 40 | $1.16 \times 10^{-4}$ | $1.19 \times 10^{-4}$ | $1.63 \times 10^{5}$ | 0.995 | $1.02 \times 10^{-2}$ | 5.149 | $6.44 \times 10^{-4}$ | 0.778 | $2.49 \times 10^{-4}$ | $1.19 \times 10^{-3}$ | 0.824 | 20.50 |

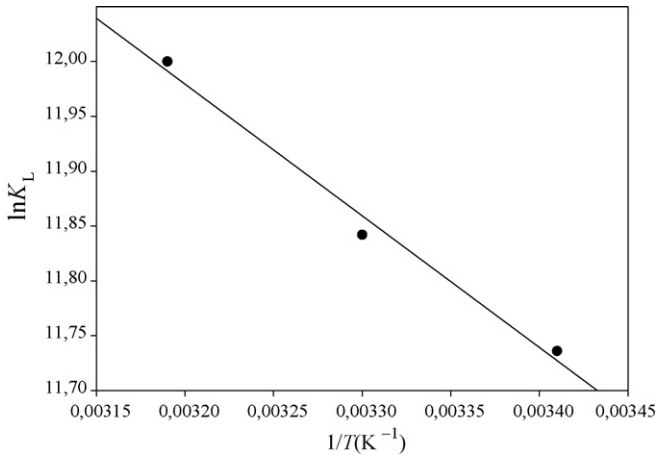


**Fig. 9.** Van't Hoff plot for the biosorption of AR44 onto *A. bisporus*.

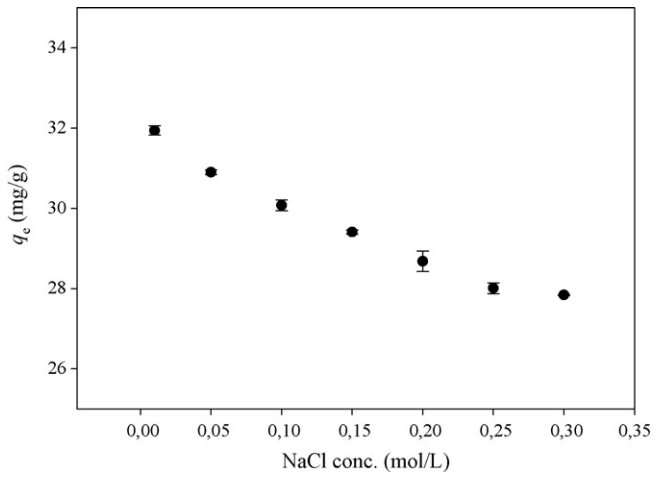


**Fig. 10.** Effect of the salt concentration on the biosorption of AR44 onto *A. bisporus* (the bars represent the standard error of the mean).

values lie between 0 and 1, the biosorption process is considered to be favorable [33,35]. In this study, we found the values of $R_L$ between $1.32 \times 10^{-2}$ and $1.02 \times 10^{-2}$, and this indicated that the biosorption of AR44 onto *A. bisporus* is favorable.

In the D–R isotherm model, the constant $\beta$ gives an idea about the mean free energy $E$ (kJ mol$^{-1}$) of biosorption can be calculated using the relationship [36]:

$$E = \frac{1}{(2\beta)^{1/2}} \quad (8)$$

The magnitude of $E$ value gives information about the biosorption mechanism as chemical ion-exchange or physical sorption. The estimated values of $E$ for AR44 biosorption was found in the range between 19.46 and 20.50 kJ mol$^{-1}$, which indicated one of the mechanisms for the biosorptive removal of AR44 by *A. bisporus* may be physical sorption.

### 3.5. Thermodynamic parameters

Thermodynamic parameters such as $\Delta H^\circ$, $\Delta G^\circ$ and $\Delta S^\circ$ for the biosorption of AR44 onto *A. bisporus* were evaluated using the following equations and can be calculated from a plot $\ln K_L$ against $1/T$ (Fig. 9):

$$\Delta G^\circ = -RT \ln K_L \quad (9)$$

$$\ln K_L = -\frac{\Delta G^\circ}{RT} = -\frac{\Delta H^\circ}{RT} + \frac{\Delta S^\circ}{R} \quad (10)$$

where $K_L$ is the Langmuir isotherm constant, $R$ is the universal gas constant (8.314 J mol$^{-1}$ K$^{-1}$) and $T$ is temperature (K).

As can be seen from Table 3, the positive value of $\Delta H^\circ$ confirms the endothermic character of AR44 biosorption whereas the negative value of $\Delta G^\circ$ indicates the spontaneity of biosorption process. Low value of $\Delta S^\circ$ indicates that no remarkable change on entropy associated to the biosorption and the positive $\Delta S^\circ$ values show the affinity of the biosorbent for an acid dye, AR44.

**Table 3**
Thermodynamic parameters calculated from Langmuir constant ($K_L$) for the biosorption of AR44 onto *A. bisporus*.

| $T$ (°C) | $\Delta G^\circ$ (kJ mol$^{-1}$) | $\Delta H^\circ$ (kJ mol$^{-1}$) | $\Delta S^\circ$ (kJ K$^{-1}$ mol$^{-1}$) |
|---|---|---|---|
| 20 | −28.427 | | |
| 30 | −29.737 | 9.976 | 0.131 |
| 40 | −31.047 | | |

### 3.6. Effect of salt

Fig. 10 presents the effect of salt concentration or ionic strength on the biosorption of AR44 by *A. bisporus*. When salt concentration was increased from 0.01 to 0.3 mol L$^{-1}$ there was a slight decrease in the biosorption capacity of biomass from 31.94 to 27.84 mg g$^{-1}$ at the optimum conditions. But even at 0.3 mol L$^{-1}$ of salt, the biosorbent still removed AR44 dye by ~80% yield. The decrease in the removal efficiency of biosorbent may also be attributed to the competition between chloride ions and dye anions for the same binding sites on the biosorbent. It was reported that generally, the biosorption mechanism of ion-exchange is ionic strength-dependent [37,38]. The adverse effect of ionic strength on dye removal may be attributed to the ion-exchange mechanism for AR44 biosorption.

### 3.7. Simulated wastewater

A simulated dye wastewater was prepared by including the known amount of AR44 (100 mg L$^{-1}$) along with the different components [39] [glucose: 0.25 g, $MgSO_4$: 0.0269 g, $FeSO_4 \cdot 7H_2O$: 0.125 g, $NiSO_4 \cdot 6H_2O$: 0.0076 g, $Na_2CO_3$: 1.25 g, $NH_4Cl$: 0.325 g, $Ca(NO_3)_2 \cdot 4H_2O$: 0.0308 g, $MnSO_4 \cdot H_2O$: 0.235 g, $ZnSO_4 \cdot 7H_2O$: 0.0021 g, $CoCl_2 \cdot 6H_2O$: 0.0016 g] dissolved in 0.25 L of tap water. The pH of the simulated water (pH ~ 7.0) was adjusted to optimum value of 2.0. The proposed biosorption procedure was applied to this sample in order to examine the matrix effect on the biosorption performance of the biosorbent. The aqueous environment deeply affects the bisorption potential of the biomass particularly in the presence of metallic species. In this study there is no considerable matrix effect caused by metal cations due to the acidic pH of the biosorption medium (pH: 2.0). Because the binding sites on the biosorbent surface were protonated at this pH value and this prevents the approach of the metal cations as a result of repulsive forces. On the other hand there is some what less dye biosorption occurred in the simulated wastewater due to the presence of other anions like $SO_4^{2-}$, $CO_3^{2-}$, $Cl^-$ and $NO_3^-$ in wastewater which occupy the dye binding sites and therefore lesser dye anion removal occurred. The biosorption yield was found as 92.4% in simulated conditions. Therefore, it may be concluded that *A. bisporus* could effectively remove AR44 dye from wastewaters.

### 3.8. Biosorbent characterization

In order to characterize the surface structure of the biosorbent, SEM micrograph was taken. The SEM image in Fig. 11 shows the

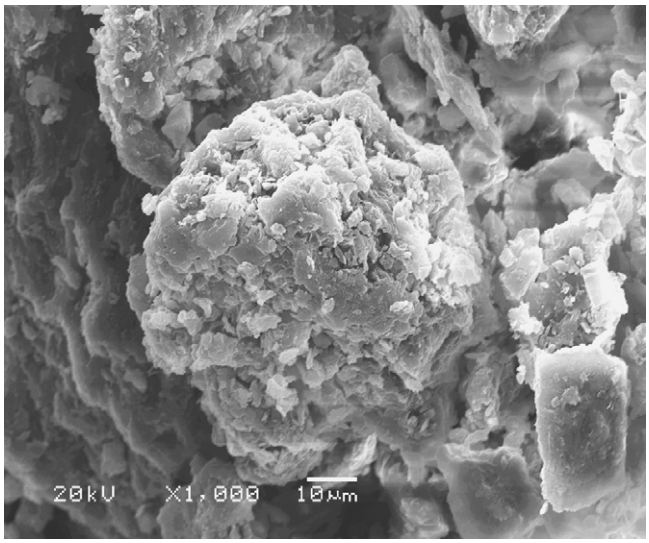


**Fig. 11.** SEM image of *A. bisporus* biomass.

morphology of biosorbent. The surface structure of the biosorbent material is uneven, heterogeneous and porous. This porous structure may be a good characteristic for possible dye–biosorbent interaction.

The existence of the functional groups on the biosorbent surface and their responsibility for dye biosorption were supported by FTIR technique. Therefore, FTIR spectra of the biosorbent before and after AR44 biosorption were taken and the band positions of the main functional groups were included in Table 4. The absorption bands of –OH and/or –NH groups were observed at 2927 $cm^{-1}$ for both samples. Two weak absorption bands at 2927 and 2855 $cm^{-1}$ show the characteristic stretching vibrations of alkyl ($CH_n$) groups on the unloaded and dye-loaded biomass. –C=O chelate stretching vibrations of amid-I band were observed at 1636 and 1640 $cm^{-1}$ for unloaded and dye-loaded biomass, respectively. An absorption band at 1560 $cm^{-1}$ in the FTIR spectrum of unloaded biomass can be attributed to amid-II band. This band slightly shifted to 1548 $cm^{-1}$ and an intensity increase was observed in the FTIR spectrum of dye-loaded biomass. The band at 1260 $cm^{-1}$ in the FTIR spectrum of unloaded biomass which is indicative of the existence of –C–O stretching shifted to a lower frequency (1230 $cm^{-1}$) after AR44 biosorption. There is no strong shifting in the absorption band at 1157 $cm^{-1}$ but the intensity of this peak slightly increased in the FTIR spectrum of dye-loaded biosorbent. Also an intensity decrease and a slight band shifting (to 1078 $cm^{-1}$) were observed in the absorption band at 1084 $cm^{-1}$ relates to –P=O stretching vibrations. Finally, new absorption bands appearing between 770 and 625 $cm^{-1}$ in the FTIR spectrum of dye-loaded biomass may be attributed to the aromatic –C–H bending vibrations in dye structure.

The changes observed in the spectrum of unloaded biomass may be an evidence for the responsibility of some functional groups on the biosorbent for AR44 biosorption.

**Table 4**
Band positions before and after AR44 biosorption by FTIR technique.

| Suggested assignment | Band positions ($cm^{-1}$) | |
|---|---|---|
| | Unloaded biomass | Dye-loaded biomass |
| –OH and/or –NH stretching | 3427 | 3427 |
| –CH symmetric stretching | 2925 | 2924 |
| –CH asymmetric stretching | 2855 | 2854 |
| Amid-I band | 1636 | 1640 |
| Amid-II band | 1560 | 1548 |
| –CH bending vibrations | 1456 | 1454 |
| –CH bending vibrations | 1378 | 1378 |
| –C–O stretching | 1260 | 1230 |
| –S=O stretching | 1157 | 1158 |
| –P=O stretching | 1084 | 1078 |
| –C–O stretching | 1025 | 1032 |
| –CH bending vibrations (aromatic) | – | 770–625 |

## 4. Conclusion

Results of this study indicate that the macro-fungus *A. bisporus* can be successfully used for the decolorization of AR44 contaminated solutions. The biosorption pattern of dye was pH-dependent. The equilibrium biosorption data were modeled using Freundlich, Langmuir and D–R isotherm equations. Kinetic studies indicated that biosorption behavior of the biosorbent was well described by the pseudo-second-order kinetic model. Thermodynamic parameters confirmed the favorable and endothermic biosorption process. Likewise, FTIR and SEM analysis were employed for the characterization of the biosorbent before and after AR44 biosorption. According to simulated wastewater studies, no considerable matrix effect was observed during the AR44 removal process. Overall, its easy availability and effectiveness of macro-fungus *A. bisporus* make it a strong choice in the investigation of an economical way of acid dye removal process.

## References

[1] O.J. Hao, H. Kim, P.C. Chiang, Decolorization of wastewater, Crit. Rev. Environ. Sci. Technol. 30 (2000) 449–505.
[2] L. Lian, L. Guo, Chunjing Guo, Adsorption of congo red from aqueous solutions onto Ca-bentonite, J. Hazard. Mater. 161 (2009) 126–131.
[3] Y. Fu, T. Viraraghavan, Fungal decolorization of wastewaters: a review, Bioresour. Technol. 79 (2001) 251–262.
[4] G. Bayramoglu, M.Y. Arica, Biosorption of benzidine based textile dyes Direct Blue 1 and Direct red 128 using native and heat treated biomass of *Trametes versicolor*, J. Hazard. Mater. 143 (2007) 135–143.
[5] R. Aravindhan, J.R. Rao, B.U. Nair, Removal of basic yellow dye from aqueous solution by sorption on green algae *Caulerpa scalpelliformis*, J. Hazard. Mater. 142 (2007) 68–76.
[6] T. Akar, I. Tosun, Z. Kaynak, E. Ozkara, O. Yeni, E.N. Sahin, S. Tunali Akar, An attractive agro-industrial by-product in environmental cleanup: dye biosorption potential of untreated olive pomace, J. Hazard. Mater. 166 (2009) 1217–1225.
[7] Z. Zhang, S. Xia, X. Wang, A. Yang, B. Xu, L. Chen, Z. Zhu, J. Zhao, N.J. Renault, D. Leonard, A novel biosorbent for dye removal: extracellular polymeric substance (EPS) of *Proteus mirabilis* TJ-1, J. Hazard. Mater. 163 (2009) 279–284.
[8] M.M. Assadi, K. Rostami, M. Shahvali, M. Azin, Decolorization of textile wastewater by *Phanerochaete chrysosporium*, Desalination 141 (2001) 331–336.
[9] T. Akar, A.S. Ozcan, S. Tunali, A. Ozcan, Biosorption of a textile dye (Acid Blue 40) by cone biomass of *Thuja orientalis*: estimation of equilibrium thermodynamic and kinetic parameters, Bioresour. Technol. 99 (2008) 3057–3065.
[10] M.M. Assadi, M.R. Jahangiri, Textile wastewater treatment by *Aspergillus niger*, Desalination 141 (2001) 1–6.
[11] J.T. Matheickal, Q. Yu, Biosorption of lead (II) from aqueous solutions by *Phellinus badius*, Miner. Eng. 10 (1997) 947–957.
[12] N.S. Maurya, A.K. Mittal, P. Cornel, E. Rother, Biosorption of dyes using dead macro fungi: effect of dye structure, ionic strength and pH, Bioresour. Technol. 97 (2006) 512–521.
[13] Z. Zulfadhly, M.D. Mashitah, S. Bhatia, Heavy metals removal in fixed-bed column by the macro fungus *Pycnoporus sanguineus*, Environ. Pollut. 112 (2001) 463–470.
[14] A.K. Mittal, S.K. Gupta, Biosorption of cationic dyes by dead macro fungus *Fomitopsis carnea*: batch studies, Water Sci. Technol. 34 (1996) 81–87.
[15] A. Sarı, M. Tüzen, Kinetic and equilibrium studies of biosorption of Pb(II) and Cd(II) from aqueous solution by macrofungus (*Amanita rubescens*) biomass, J. Hazard. Mater. 164 (2009) 1004–1011.
[16] N. Ertugay, Y.K. Bayhan, Biosorption of Cr(VI) from aqueous solutions by biomass of *Agaricus bisporus*, J. Hazard. Mater. 154 (2008) 432–439.
[17] M.A. Garcia, J. Alonso, M.J. Melgar, *Agaricus macrosporus* as a potential bioremediation agent for substrates contaminated with heavy metals, J. Chem. Technol. Biotechnol. 80 (2005) 325–330.
[18] M.J. Melgar, J. Alonso, M.A. Garcia, Removal of toxic metals from aqueous solutions by fungal biomass of *Agaricus macrosporus*, Sci. Total Environ. 385 (2007) 12–19.
[19] T. Akar, B. Anilan, Z. Kaynak, A. Gorgulu, S. Tunali Akar, Batch and dynamic flow biosorption potential of *Agaricus bisporus*/*Thuja orientalis* biomass mixture for decolorization of RR45 dye, Ind. Eng. Chem. Res. 47 (2008) 9715–9723.

[20] S. Tunali Akar, A. Gorgulu, Z. Kaynak, B. Anilan, T. Akar, Biosorption of Reactive Blue 49 dye under batch and continuous mode using a mixed biosorbent of macro fungus *Agaricus bisporus* and *Thuja orientalis* cones, Chem. Eng. J. 148 (2009) 26–34.
[21] Z. Aksu, A.I. Tatlı, Ö. Tunç, A comparative adsorption/biosorption study of Acid Blue 161: effect of temperature on equilibrium and kinetic parameters, Chem. Eng. J. 142 (2008) 23–39.
[22] B.E. Wang, Y.Y. Hu, L. Xie, K. Peng, Biosorption behavior of azo dye by inactive CMC immobilized *Aspergillus fumigatus* beads, Bioresour. Technol. 99 (2008) 794–800.
[23] R. Gong, Y. Jin, F. Chen, J. Chen, Z. Liu, Enhanced malachite green removal from aqueous solution by citric acid modified rice straw, J. Hazard. Mater. 137 (2006) 865–870.
[24] R. Gong, Y. Jin, J. Chen, Y. Hu, J. Sun, Removal of basic dyes from aqueous solution by sorption on phosphoric acid modified rice straw, Dyes Pigments 73 (2007) 332–337.
[25] Y.S. Ho, J.C.Y. Ng, G. McKay, Kinetics of pollutant sorption by biosorbents: review, Sep. Purif. Methods 29 (2000) 189–232.
[26] S. Lagergren, Zur theorie der sogenannten adsorption gelöster stoffe Kungliga Svenska Vetenskapsakademiens, Handlingar 24 (1898) 1–39.
[27] Y.S. Ho, G. McKay, Kinetic models for the sorption of dye from aqueous solution by wood, Process Saf. Environ. Prot. 76 (B2) (1998) 183–191.
[28] H.M.F. Freundlich, Über die adsorption in lösungen, Z. Phys. Chem. 57 (1906) 385–470.
[29] I. Langmuir, The adsorption of gases on plane surfaces of glass, mica and platinium, J. Am. Chem. Soc. 40 (1918) 1361–1403.
[30] M.M. Dubinin, L.V. Radushkevich, Proc. Acad. Sci. U.S.S.R. Phys. Chem. Sect. 55 (1947) 331–333.
[31] Y. Liu, Y.-J. Liu, Biosorption isotherms, kinetics and thermodynamics, Sep. Purif. Technol. 61 (2008) 229–242.
[32] B.H. Hameed, Equilibrium and kinetic studies of methyl violet sorption by agricultural waste, J. Hazard. Mater. 154 (2008) 204–212.
[33] K.R. Hall, L.C. Eagleton, A. Acrivos, T. Vermeulen, Pore-and solid diffusion kinetics in fixed-bed adsorption under constant-pattern conditions, Ind. Eng. Chem. Fundam. 5 (1966) 212–223.
[34] R. Nadeem, M.A. Hanif, F. Shaheen, S. Perveen, M.N. Zafar, T. Iqbal, Physical and chemical modification of distillery sludge for Pb(II) biosorption, J. Hazard. Mater. 150 (2008) 335–342.
[35] T.W. Weber, R.K. Chakravorti, Pore and solid diffusion models for fixed-bed adsorbers, J. Am. Inst. Chem. Eng. 20 (2) (1974) 228–238.
[36] S.M. Hasany, M.H. Chaudhary, Sorption potential of Hare River sand for the removal of antimony from acidic aqueous solution, Appl. Radiat. Isot. 47 (4) (1996) 467–471.
[37] E. Pehlivan, B.H. Yanık, G. Ahmetli, M. Pehlivan, Equilibrium isotherm studies for the uptake of cadmium and lead ions onto sugar beet pulp, Bioresour. Technol. 99 (2008) 3520–3527.
[38] D. Xu, X. Tan, C. Chen, X. Wang, Removal of Pb(II) from aqueous solution by oxidized multiwalled carbon nanotubes, J. Hazard. Mater. 154 (2008) 407–416.
[39] S.V. Mohan, N. Chandrasekhara Rao, P.N. Sarma, Simulated acid azo dye (Acid black 210) wastewater treatment by periodic discontinuous batch mode operation under anoxic–aerobic–anoxic microenvironment conditions, Ecol. Eng. 31 (2007) 242–250.